

KAWASAKI STEEL TECHNICAL REPORT

No.26 (June 1992)

Artificial Intelligence and Wire Rods and Steel Bars

Effect of Alloying Elements on Cold Forgeability of 0.53%C Steel

Toshiyuki Hoshino, Keniti Amano, Nobuhisa Tabata, Shozaburo Nakano

Synopsis :

The effects of alloying elements on both forgeability and hardenability were investigated in order to apply a 0.53 mass% C steel to cold forging use. The deformation resistance of a spheroidized 0.53 mass% C steel by applying the cold forging increased with alloying elements in the order of silicon, manganese, chromium, and molybdenum. The addition of silicon reduced the formability and increased the deformation resistance even in an amount as small as 0.1 mass%. The effects of manganese, chromium, and molybdenum on the formability were closely related to the change in morphology of spheroidized carbides. The hardening depth of the spheroidized steel by induction hardening was controlled by adjusting the amounts of manganese, molybdenum, and silicon. Chromium decreased the hardening depth of the spheroidized steel, since chromium atoms were dissolved into cementite during spheroidizing annealing, resulting in stabilizing the cementite. In this case, the cementite was not fully dissolved in the austenite phase by rapid induction heating. The 0.53 mass% C steel can be applied to cold forging use by optimizing the chemical composition of the steel on the basis of these results.

(c)JFE Steel Corporation, 2003

The body can be viewed from the next page.

Effect of Alloying Elements on Cold Forgeability of 0.53%C Steel*



Toshiyuki Hoshino
Senior Researcher,
Plate, Shape & Casting
Lab., Heavy Steel
Products Res. Dept.,
Iron & Steel Res.
Labs.



Keniti Amano
Dr. Engi., Chief of
Plate, Shape &
Casting Lab., Heavy
Steel Products Res.
Dept., Iron & Steel
Res. Labs.



Nobuhisa Tabata
Senior Researcher,
Joining & Physical
Metallurgy Lab., Heavy
Steel products Res.
Dept., Iron & Steel
Res. Labs.



Shozaburo Nakano
Chief of Construction
Engineering Lab.,
Structure Res. Labs.,
Engineering &
Construction Div.

1 Introduction

Cold forging has been widely applied to the manufacture of many machine parts to achieve minimum material consumption, high productivity, and accurate dimensions. It can also eliminate part of machining process from a manufacturing of machine parts including a hot forging. Cold forging has been applied to bigger and more complicatedly shaped parts due to improvement in forging machines in terms of their load capacity and deformation rate.¹⁻³⁾

The required properties of a steel for cold forging use become more stringent as the cold forging technique

Synopsis:

The effects of alloying elements on both forgeability and hardenability were investigated in order to apply a 0.53 mass% C steel to cold forging use. The deformation resistance of a spheroidized 0.53 mass% C steel by applying the cold forging increased with alloying elements in the order of silicon, manganese, chromium, and molybdenum. The addition of silicon reduced the formability and increased the deformation resistance even in an amount as small as 0.1 mass%. The effects of manganese, chromium, and molybdenum on the formability were closely related to the change in morphology of spheroidized carbides. The hardening depth of the spheroidized steel by induction hardening was controlled by adjusting the amounts of manganese, molybdenum, and silicon. Chromium decreased the hardening depth of the spheroidized steel, since chromium atoms were dissolved into cementite during spheroidizing annealing, resulting in stabilizing the cementite. In this case, the cementite was not fully dissolved in the austenite phase by rapid induction heating. The 0.53 mass% C steel can be applied to cold forging use by optimizing the chemical composition of the steel on the basis of these results.

improves. Since low cold-deformation resistance and high hardenability are generally required of a steel for cold forging use, the decrease of nonmetallic inclusions and the elimination of surface scratches in hot-rolled steel bar of original materials are needed.⁴⁾

Either carbon or low-alloy steel containing less than 0.45 mass% and under carbon has been conventionally used for cold forging, since steel containing above 0.45%C has markedly shortened the life of dies.

More recently, it has been required that the cold forging of a steel containing above 0.45%C can be applied to a manufacturing process of machine parts in terms of replacing a carburizing to an induction heating followed by quenching (induction hardening),⁵⁾ which saves energy and increases productivity. There are, however, few studies concerning the cold forgeability of steel containing above 0.45%C.⁶⁾

In this study, the effects of alloying elements on both forgeability and hardenability were investigated in order to apply a 0.53%C steel to cold forging use.

* Originally published in *Kawasaki Steel Giho*, 23(1991)2, 105-111

2 Experimental Methods

2.1 Materials

Vacuum melted steels with the chemical compositions shown in **Table 1** were used. Steels A1 to A4 had differing Si content in the 0.53%C–0.75%Mn–0.15%Cr steel. Steels B1 to B3, C1 and C2, and D1 to D3 had differing contents of Mn, Mo, and Cr of the 0.53%C–0.01%Si steel. All steels were tested to investigate the effect of these elements, which are effective for hardenability, on cold forgeability. JIS grades S30C and S45C, which are usually applied to the manufacture of machine parts by cold forging, were used as comparison. These steels were hot-forged into 35 mm diameter bars, normalized at 850°C for 60 min, and then conducted the spheroidizing annealing whose heat cycle is shown in **Fig. 1**.

2.2 Microstructural Observation

The microstructure of a longitudinal section of each spheroidized steel etched by nital was observed using optical and scanning-electron microscopes.

The diameter, volume fraction, aspect ratio of carbides, and spheroidizing ratio were measured from the scanning-electron micrograph of each steel by using an image analyzer. Here, the aspect ratio of a carbide means the ratio of the longest carbide diameter to the shortest one. The ratio of the number of carbides whose aspect ratio was not more than 2 to the total number of carbides was defined as the spheroidizing ratio.

2.3 Cold Forgeability Test

Cylindrical specimens of 15 mm in diameter and 22.5 mm in height were machined from the spheroidized steels. A cold upsetting test was then conducted in a press machine with load capacity of 2.94×10^6 N, both ends of each specimen being constrained by circularly grooved dies during the test. The strain rate in the initial stage of deformation was 8.8 s^{-1} .

The cold deformation resistance was calculated from the measured load during the cold upsetting test by using the method proposed by Osakada et al.⁷⁾ The limiting upsetting ratio was defined as the reduction in height at which the fraction of visually observed cracked specimens became 50%.

2.4 Hardness Measurement

The hardness of the longitudinal section of each spheroidized steel was measured with a Vickers hardness tester with a load of 98.07N, the hardness of the matrix ferrite phase itself being measured with a microhardness tester with a load of 0.029N.

2.5 Induction Hardening Test

Because a 0.53%C steel, after forming into an intended shape, is usually case-hardened by an induction

Table 1 Chemical compositions of steels (mass%)

steel	C	Si	Mn	P	S	Cr	Mo	Al	N
A1	0.53	0.02	0.75	0.016	0.010	0.16	—	0.043	0.0057
A2	0.53	0.10	0.76	0.016	0.010	0.16	—	0.044	0.0058
A3	0.54	0.22	0.75	0.016	0.009	0.15	—	0.046	0.0063
A4	0.53	0.49	0.74	0.015	0.010	0.15	—	0.044	0.0067
B1	0.53	0.01	0.29	0.005	0.008	—	—	0.046	0.0036
B2	0.53	0.01	0.50	0.008	0.009	—	—	0.043	0.0040
B3	0.53	0.01	0.75	0.009	0.010	—	—	0.041	0.0052
C1	0.53	0.01	0.48	0.008	0.010	—	0.1	0.040	0.0041
C2	0.52	0.01	0.48	0.006	0.009	—	0.3	0.049	0.0042
D1	0.53	0.01	0.49	0.006	0.009	0.15	0.1	0.048	0.0056
D2	0.53	0.01	0.47	0.006	0.010	0.29	0.1	0.048	0.0045
D3	0.53	0.01	0.49	0.005	0.009	0.70	0.1	0.048	0.0047
S30C	0.29	0.22	0.75	0.016	0.010	0.18	—	0.044	0.0061
S45C	0.47	0.22	0.75	0.017	0.009	0.17	—	0.045	0.0059

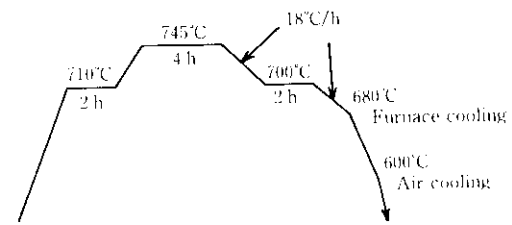


Fig. 1 Schematic diagram of spheroidizing annealing

hardening in order to improve the fatigue life and the wear resistance, the induction hardenability of each steel was investigated in this study.

Specimens of 30 mm in diameter and 100 mm in length were machined from each steel after normalizing and/or spheroidizing annealing. The induction hardening was performed with a migrating induction heating device of a frequency of 15 kHz; the electric power of the device, its cathode voltage, and the speed of workpieces were set to 114 kW, 9.5 kV, and 6 mm/s, respectively. The surface temperature of the specimens during induction heating was 1075°C. Each specimen was then water-quenched and tempered at 150°C for 60 min, before the hardness distribution of the cross section was measured. The distance of the point at which the hardness reached Hv 392 from the surface of a specimen was defined as the effective hardening depth.

3 Experimental Results

3.1 Microstructure

The microstructure of the normalized steel was ferrite and pearlite. Scanning electron-micrographs of the

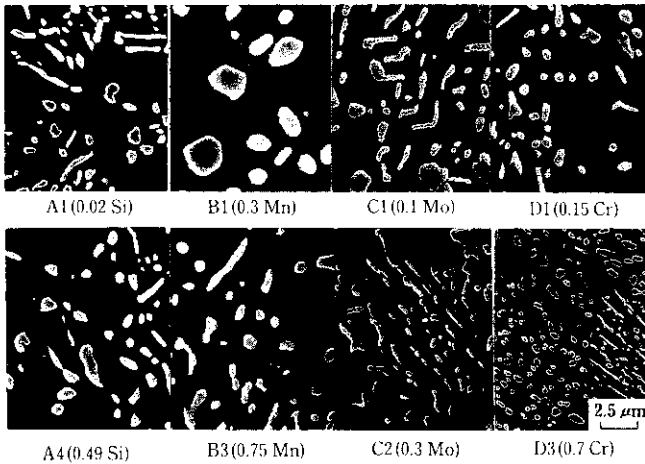


Photo 1 Electron micrographs after spheroidizing annealing of steels examined

spheroidized steels are shown in **Photo 1**. Increasing the Si content (series A) scarcely affected the carbide morphology. On the other hand, the carbides in the spheroidized steels of series B, C, and D with various contents of Mn, Mo, and Cr, respectively, became finer with increasing alloying elements.

The relationship between the Si content and microstructural parameters of the steels is shown in **Fig. 2**. Spheroidizing ratio S_{ra} was improved with increasing Si content. Diameter of cementite, D_{cem} , volume fraction of cementite, V_{cem} , and ferrite grain size D_a were approxi-

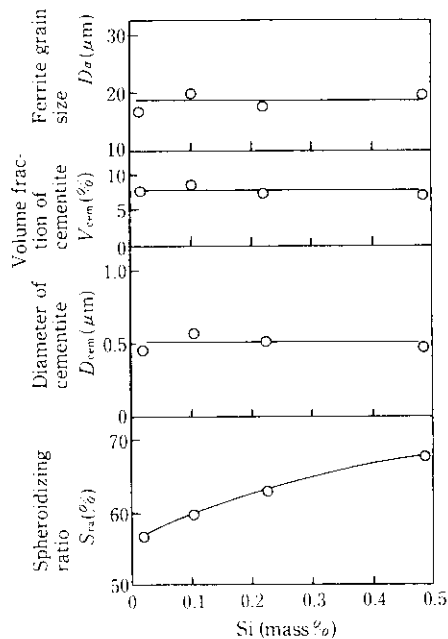


Fig. 2 Relation between silicon content and structural parameters such as S_{ra} , D_{cem} , V_{cem} and D_a of steels A1 to A4 after spheroidizing annealing

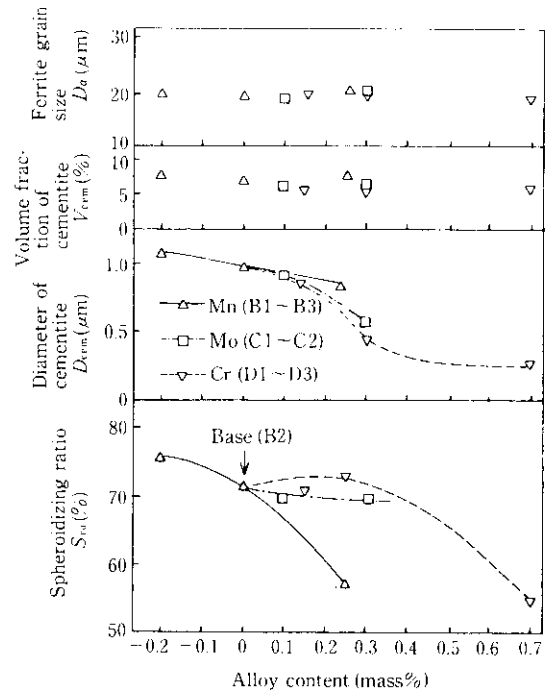


Fig. 3 Variation of structural parameters such as S_{ra} , D_{cem} , V_{cem} , and D_a of steels after spheroidizing annealing with change in contents of various alloying elements on the basis of steel B2

mately constant at $0.5 \mu\text{m}$, 8%, and $20 \mu\text{m}$, respectively.

Figure 3 shows the variation of micro-structural parameters after spheroidizing annealing of the steels of series B, C, and D. The alloying content on the x-axis in **Fig. 3** means the change in content compared to steel B2 containing 0.53%C–0.01%Si–0.5%Mn. The spheroidizing ratios of steels B3 and D3 containing 0.75%Mn and 0.70%Cr, respectively, were reduced to approximately 55%, while those of the other steels were roughly 70%. Steel B1 containing 0.3%Mn had the highest ratio of 76%.

The cementite diameter of all steels decreased with increasing alloying content; in particular, this phenomenon was significant in the Cr- and Mo-bearing steels. The volume fraction of cementites and the ferrite grain size in the matrix phase were independent of alloying contents at 8% and $20 \mu\text{m}$, respectively.

3.2 Cold Forgeability Test

The variation in deformation resistance and the fraction of cracking of spheroidized S30C and S45C, which were used for comparison, with the average strain in the cold upsetting test are shown in **Fig. 4**. S30C steel showed lower cold deformation resistance, and higher limiting upsetting ratio than those of the S45C steel.

The deformation resistance at an average strain of 1.08 and the limiting upsetting ratio of steels A1 to A4 in the cold forging test are plotted in **Fig. 5** as a function of Si content. An increase in Si content from 0.02% to 0.49% raised the cold deformation resistance

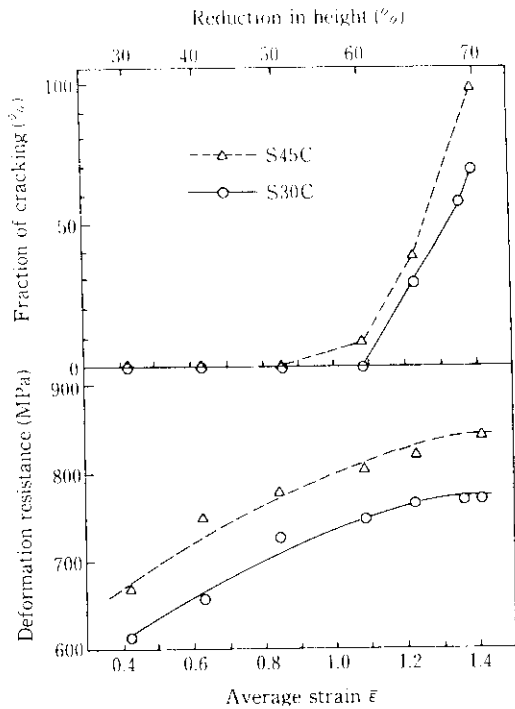


Fig. 4 Variation of both deformation resistance and the fraction of cracking of spheroidized S30C and S45C steels with average strain during the cold forging test (The fraction of cracking means the percentage of cracked specimens in the ten specimens that were deformed by the same average strain.)

by about 70 MPa. The addition of Si, even in such a small amount as 0.1%, significantly increased the deformation resistance. It should be noted that a decrease in Si content is effective for lowering the deformation resistance during cold forging.

The limiting upsetting ratio decreased with increasing Si content in the steels as shown in Fig. 5. The limiting upsetting ratio for 0.49%Si steel was 7% lower than that for 0.02%Si steel. Steel A3 containing 0.22%Si, which corresponds to JIS grade S53C, had a deformation resistance 6 to 12% higher and a limiting upsetting ratio 6 to 9% lower than the figures for S30C and S45C steels. This means that applying a conventional 0.53%C steel to cold forging is quite difficult.

Figure 6 shows the effects of Mn, Mo, and Cr on the deformation resistance at an average strain of 1.08 and the limiting upsetting ratio of steel B2. Raising the content of Mn and Cr increased the deformation resistance of the spheroidized steels.

The influence of Mo on the deformation resistance was lower than that of Mn and Cr. If a comparison is made of the increase in deformation resistance at the maximum content of an alloying element, the increase in deformation resistance associated with the addition of alloying elements is in the order of Si, Mn, Cr, and Mo.

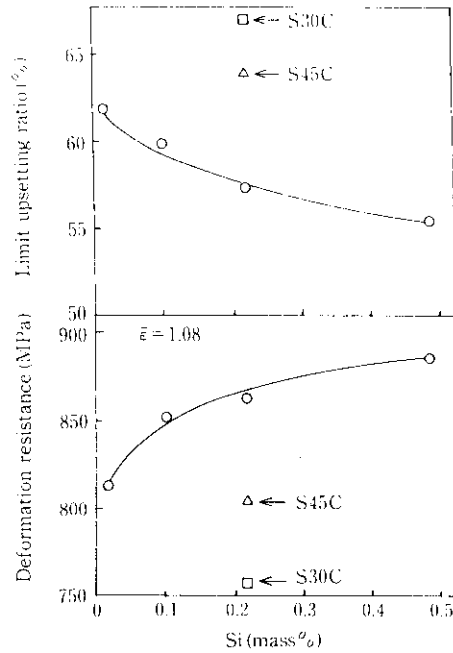


Fig. 5 Changes in both deformation resistance at average strain ($\bar{\epsilon}$) of 1.08 and the limit upsetting ratio of steels A1 to A4 after spheroidizing annealing in the cold forging test as a function of silicon content (The limit upsetting ratio means the reduction in height that the fraction of cracking of the specimen reaches fifty percent.)

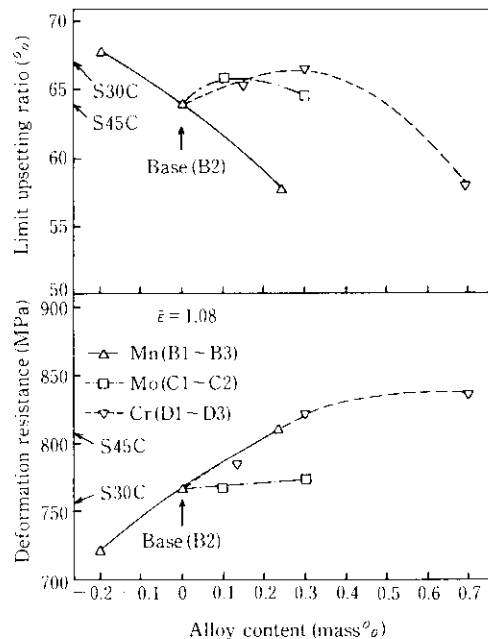


Fig. 6 Variations of both deformation resistance at average strain ($\bar{\epsilon}$) of 1.08 and the limit upsetting ratio of steels after spheroidizing annealing with change of various alloying elements on the basis of steel B2

The limiting upsetting ratio of steel B1 containing 0.3%Mn was highest at 68%. However, as the Mn content was increased to 0.7%, the limiting upsetting ratio lowered.

Neither Mo nor Cr affected the limiting upsetting ratio, apart from steel D3 containing 0.7%Cr. The deformation resistance of all the steels, except for steel D3 containing 0.7%C, was lower than that of S45C steel. In particular, the deformation resistance of steel B1 with a 0.3%Mn content was the lowest, which was lower even than that of S30C steel. On the other hand, the limiting upsetting ratios of all the steels, apart from B3 and D3 containing 0.75%Mn and 0.7%Cr, respectively, were higher than the value for S45C steel.

These results show that, if the chemical composition of the steel is suitably designed, it is possible for high-carbon steel containing 0.53%C to have equivalent cold forgeability to that of S45C steel.

3.3 Hardness

The effects of the alloying elements on the hardness of spheroidized steels are shown in Fig. 7. The addition of Si raised both the hardness of the overall phase and that of the ferrite phase. This means that the hardness of the overall phase depended on the solid solution strengthening of ferrite by Si.

Mn increased the hardness of the ferrite phase as well as Si did. In the Cr- and Mo-bearing steels, the behavior of the hardness of the overall phase with the alloying content was different from that of the ferrite phase. These results suggest that other controlling factors besides solid solution strengthening of the matrix ferrite phase affected the hardness of the overall phase.

3.4 Induction Hardenability

Figure 8 illustrates the relationship between the ideal critical diameter (DI) and the effective hardening depth for the normalized and spheroidized steels after induction heating and subsequent quenching and tempering. The DI value was calculated from Eq. (1).⁸⁾

$$DI = 0.338 \times \sqrt{C}(1 + 0.64Si)(1 + 4.1Mn)(1 + 2.83P) \\ \times (1 - 0.62S)(1 + 2.33Cr)(1 + 0.52Ni) \\ \times (1 + 3.14Mo)(1 + 0.27Cu) \times 25.4 \dots\dots(1)$$

The hardening depth in the normalized steels after induction hardening increased with increasing DI value. On the other hand, the effective hardening depth in the spheroidized steels after induction hardening was less than that of the normalized steels, depending on the alloying elements.

A decrease in effective hardening depth by changing the heat treatment before induction hardening was most distinctly observed with steels D1 to D3; the hardening depth in these spheroidized steels decreased to a figures as low as 0.9 to 1.9 mm when compared to the figures for normalized steels with increasing Cr content. It should be noted that a small addition of Cr such as

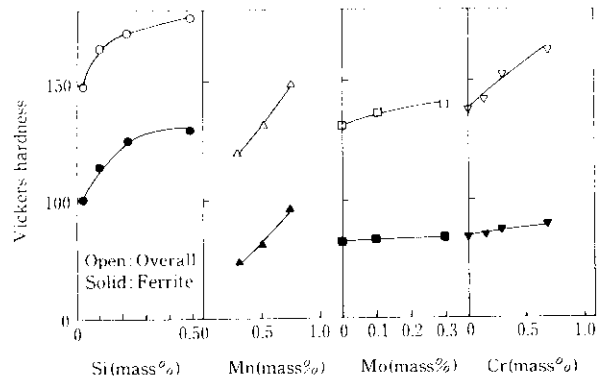


Fig. 7 Effects of content of various alloying elements on the overall hardness and local ferrite-phase hardnesses of spheroidized steels

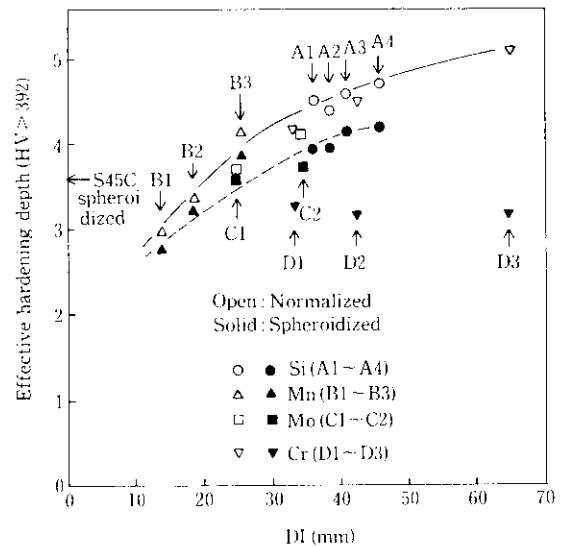


Fig. 8 Variation of the hardening depth of normalized and spheroidized steels after the induction heating and quenching with the ideal critical diameter (DI) calculated from the chemical compositions of steels

0.15% decreased the hardening depth.

The heat treatment before induction hardening had less effect on the hardening depths in the Si-, Mn-, and Mo-bearing steels than on those of the chromium-bearing steels. The hardening depths of steels A1 to A3, B3, and C1 to C3 after induction hardening were not less than that of S45C steel.

The hardenability of a steel is usually calculated from its chemical composition. These results, however, indicate that, if induction hardening is applied for case-hardening purposes, it is important to optimize the chemical composition of the steel depending on the heat treatment before induction hardening.

4 Discussion

4.1 Effect of the Chemical Composition of Spheroidized Steels on the Cold Deformation Resistance

The carbide volume fraction of a spheroidized steel, the diameter of a spheroidized carbide, the ferrite grain size of the matrix phase in a spheroidized steel, and the total content of alloying elements in the solution in a ferrite of a spheroidized steel can be considered as controlling factors for the cold deformation resistance of spheroidized steel⁹⁾ during cold forging. It is well known that the alloying elements in a spheroidized steel are partitioned between a spheroidized cementite and a matrix ferrite phase. Sato et al.¹⁰⁾ have investigated the partitioning of alloying elements in spheroidized steel between the spheroidized cementites and matrix ferrite phase, and proposed Eq. (2).

$$\left. \begin{aligned} \frac{[\text{Cr}]}{\text{Cr}} &= \frac{1}{1 + 4C} \\ \frac{[\text{Mn}]}{\text{Mn}} &= \frac{1}{1 + 1.4C} \\ \frac{[\text{Mo}]}{\text{Mo}} &= \frac{1}{1 + C} \\ \frac{[\text{Si}]}{\text{Si}} &= \frac{6.7}{6.7 - C} \end{aligned} \right\} \dots \dots \dots (2)$$

where [Cr], [Mn], [Mo], and [Si] represent the contents of chromium, manganese, molybdenum, and silicon in solid solution in the ferrite phase of the spheroidized steel, and Cr, Mn, Mo, and Si denote the amounts added.

If it is assumed that the effect of alloying elements on solid solution strengthening can be represented by a summation¹¹⁾ of the effect of each alloying element, the content of alloying elements in a solid solution (AS) in the ferrite phase of a spheroidized steel can be calculated by Eq. (3).

$$\text{AS} = [\text{Cr}] + [\text{Mn}] + [\text{Mo}] + [\text{Si}] \dots \dots \dots (3)$$

Figure 9 shows the variation of deformation resistance at an average strain of 1.08 in the cold forging test with the sum of the content of each alloying element in solution in the ferrite phase. The correlation between AS and the deformation resistance is so good that the sum of the content of each alloying element in solid solution is a significant factor for cold deformation resistance.

The relationship between the diameter of the spheroidized carbides and the cold deformation resistance is shown in Fig. 10. The cold deformation resistance has a tendency to decrease with increasing diameter of carbides, and the diameter of the carbides is thus one of the controlling factors for cold deformation resistance.

On the other hand, since both the volume fraction of carbides and the ferrite grain size in all the steels after

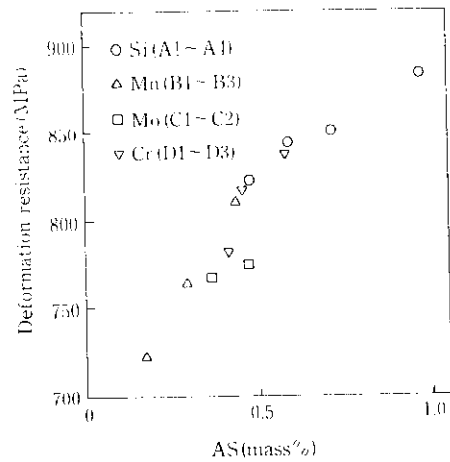


Fig. 9 Variation of deformation resistance of spheroidized steels at average strain ($\bar{\epsilon}$) of 1.08 in the cold forging test with the sum of content of alloying elements in solution (AS) in ferrite of spheroidized steel

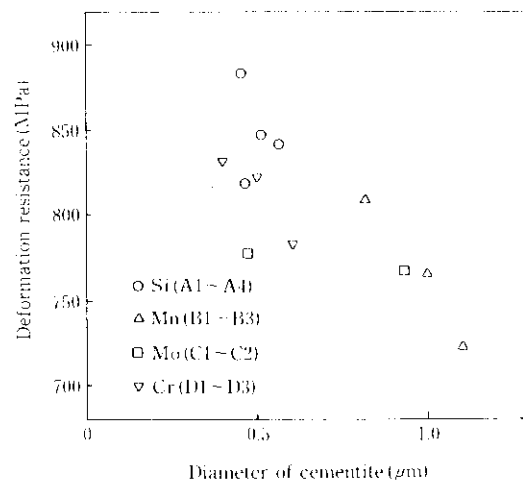


Fig. 10 Relation between the diameter of cementite of spheroidized steels and the deformation resistance at average strain ($\bar{\epsilon}$) of 1.08 during the cold forging test

spheroidizing annealing were constant at 8% and 20 μm , respectively, these parameters are not controlling factors for cold deformation resistance.

Shiozaki¹²⁾ has found that there was a good correlation between the hardness and cold deformation resistance as measured with the same upsetting test as that used in this study.

In order to clarify the contribution from solid solution strengthening and carbide refinement to cold deformation resistance, the increment in hardness was analyzed. Figure 11 shows the effects of alloying elements on the contribution from solid solution strengthening and carbide refinement to hardness. If it is assumed that the increment (shown by the obliquely hatched lines in

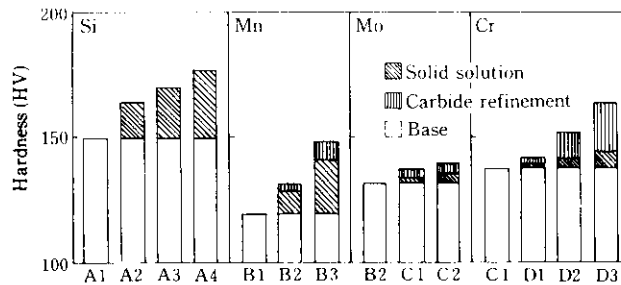


Fig. 11 Effects of alloying elements on contribution of various factors to hardness of spheroidized steels

the bar graph) in hardness of the ferrite phase was due to solid solution strengthening, the difference (vertically hatched lines) between the increment in hardness of the overall phase and that of the ferrite phase can be attributed to carbide refinement.

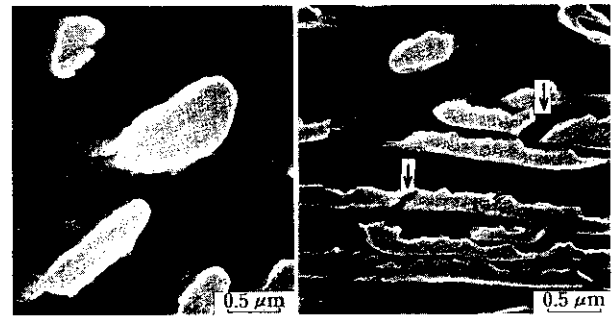
The increment in hardness of the overall phase by addition of Si was due to solid solution strengthening. On the contrary, carbide refinement contributed to the increment in hardness of the Mn-, Mo-, and Cr-bearing steels. In particular, carbide refinement was most clearly distinguished in the Cr-bearing steels. Kawakami et al.¹³⁾ have found that the cold deformation resistance of 0.04% carbon steel during cold forging decreased with increasing addition of Cr, which is the opposite result to that in our study. This would be attributable to a difference in carbide quantity; the spheroidized 0.53% carbon steel is thought to have contained more carbides than the 0.04% carbon steel.

4.2 Effects of Carbide Morphology on the Limiting Upsetting Ratio

The volume fraction and the morphology of the carbides are important factors for determining the ductility of a spheroidized steel. Edleson et al.¹⁴⁾ have investigated experimentally the relationship between the volume fraction of the second phase and ductile fracture, and indicated that the latter was dominated by the former. Furthermore, Gladman et al.¹⁵⁾ have found that the ductile fracture of a steel was changed by the morphology of the carbides, even with the same volume fraction of carbides.

In this study, the steels with the lower content of C showed the higher limiting upsetting ratio. It was also observed that the limiting upsetting ratio of the 0.53%C steels after spheroidizing annealing was different even with the same volume fraction of carbides.

Electron-micrographs of spheroidized steel A3 given an average strain of 0.62 by cold forging are shown in Photo 2. In spite of no macroscopic defects being observed on the surface under this forging condition, micro-cracks were observed at the interface between the rod-like carbide and ferrite. On the other hand, no microcracks were seen when the carbides were more



(a) Spheroidal carbide

(b) Rod-like carbide

Photo 2 Electron-micrographs of the spheroidized steel A3 given an average strain of 0.62 in the cold forging test (a: No micro-crack is observed in the neighbourhood of spheroidal carbides. b: Micro-cracks are observed in the interface of the rod-like carbide and the ferrite.)

spheroidal. It is considered that the micro-cracks formed at the interface between the carbide and ferrite were extended and connected with each other when many rod-like carbides existed during cold upsetting, which would lead to macroscopic defects. Therefore, it can be concluded that the morphology of the carbides is one of the controlling factors for the limiting upsetting ratio of a spheroidized steel.

The relationship between the spheroidizing ratio and the limiting upsetting ratio is shown in Fig. 12. With the steels of series B, C, and D, the limiting upsetting ratio increased with increasing spheroidizing ratio. On the other hand, the limiting upsetting ratio of the Si-bearing steels decreased with increasing Si content, in spite of improving the spheroidizing ratio. It is well-known that the addition of Si decreases the ductility of steel. It can be considered that the decrease in ferrite phase ductility by adding silicon accelerates the process of extending and connecting the micro-cracks that occur in the early stage of cold forging.

It can also be considered that Mn, Cr, and Mo influence the limiting upsetting ratio through the change in morphology of the carbides. It is generally known that

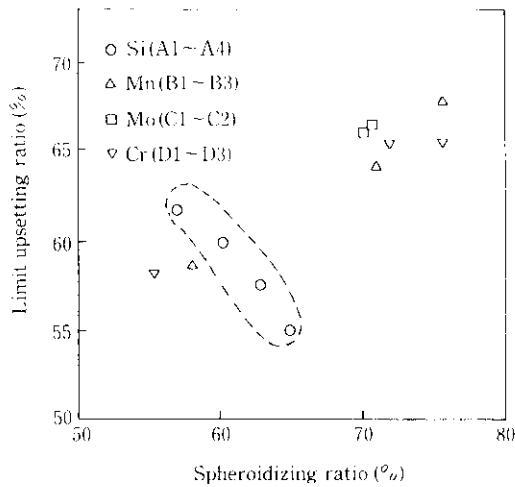


Fig. 12 Relation between spheroidizing ratio of spheroidized steels and the limit upsetting ratio in the cold forging test

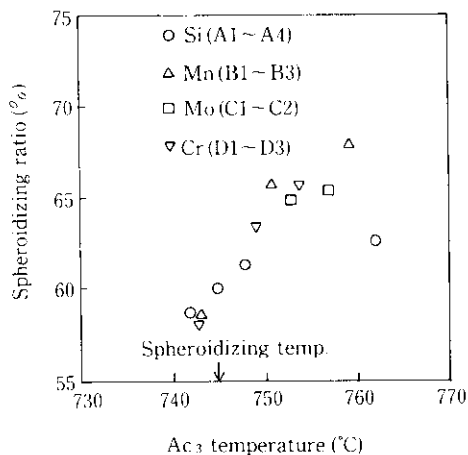


Fig. 13 Relation between A_{c3} temperature of steels and spheroidizing ratio of spheroidized steels

an undissolved carbide plays an important role in the formation of a spheroidized structure by the slow-cooling method.¹⁶⁾ If the temperature of an austenitizing process is so high as to decrease the undissolved carbide, which is the precipitation site for spheroidized carbides, rod-like carbides will increase. In view of this point, the A_{c3} temperatures of each steel were measured by using a thermal expansion test with a heating rate of $3^{\circ}\text{C}/\text{min}$. The relationship between the A_{c3} temperature and spheroidizing ratio is shown in Fig. 13. As the A_{c3} temperature became higher, the spheroidizing ratio also increased. The spheroidizing ratios of the steels containing Mn and Cr were lower, because the heating temperature became relatively higher by the addition of these elements, resulting in a decrease in the number of undissolved carbides which were precipitation sites for the spheroidized carbides. On the other hand, the spheroidizing ratios of the steels containing Mo and Si, which raise the A_{c3} temperature, were higher than those of the Mn- and Cr-bearing steels because of the remaining number of undissolved carbides.

roidizing ratios of the steels containing Mo and Si, which raise the A_{c3} temperature, were higher than those of the Mn- and Cr-bearing steels because of the remaining number of undissolved carbides.

4.3 Effect of Chemical Composition on Induction Hardenability

The effect of the heat treatment before induction hardening on the effective hardening depth was observed for all the steels examined, this phenomenon being more clearly distinguishable with the Cr-bearing steels.

An electron micrograph of spheroidized steel D3 after induction hardening and the result of an EDX analysis of the undissolved carbides are shown in Photo 3. Many undissolved carbides can be seen in the spheroidized Cr-bearing steel after induction hardening, despite the diameter of the spheroidized carbide of these steels after spheroidizing annealing being smaller than that of the other steels. According to the EDX analysis of the undissolved carbides after induction hardening, dissolution of chromium atoms into the carbide was observed, and it can thus be considered that these were cementites such as $(\text{Fe}, \text{Cr})_7\text{C}_3$.¹⁷⁾ Sato et al.¹⁰⁾ have found that a large amount of chromium atoms was dissolved into cementite by spheroidizing annealing. Furthermore, Nishizawa¹⁸⁾ has clarified that the cementite became thermodynamically stable by substitution of the iron atoms in the cementite with chromium atoms. The results in this study can be explained as follows: Cr decreases the hardening depth of spheroidized steel, since Cr atoms are dissolved into cementite during spheroidizing annealing, thus stabilizing the cementite, and not fully dissolved in the austenite phase by rapid induction heating. On the other hand, the effect of the heat treatment prior to induction hardening on the effective hardening depth of steels containing Mn, Si, and Mo was less clear than that of the Cr-bearing steels, because Mn and Mo atoms dissolved in the cementite less than Cr did, and Si atoms did not dissolve in the cementite. In this case, the addition of these elements

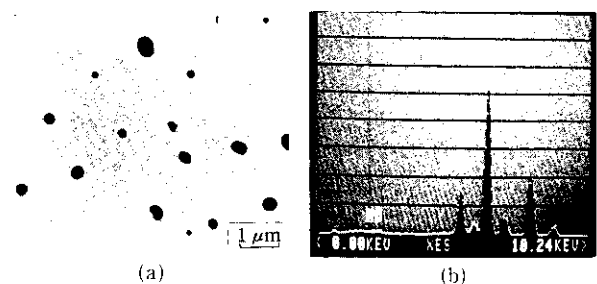


Photo 3 Electron micrograph of spheroidized steel D3 after the induction heating and quenching (a) and results of the EDX analysis of undissolved carbide (b)

would not affect the behavior of cementite dissolution into an austenite phase even with rapid induction heating.

5 Conclusions

The effects of adding Si, Mn, Cr, and Mo on both the cold forgeability and hardenability of 0.53%C steel were investigated in order to apply this material for cold forging use. The results obtained are as follows:

- (1) The deformation resistance of spheroidized 0.53%C steel was increased with increasing amount of alloying elements in the order of Si, Mn, Cr, and Mo. Si increased the deformation resistance even by a small addition of 0.1%.
- (2) The deformation resistance of spheroidized 0.53% steel was controlled by both solid solution strengthening of the ferrite phase and carbide refinement. Si increased the deformation resistance through solid solution strengthening of the ferrite phase. On the other hand, Mn, Cr, and Mo increased the deformation resistance through both solid solution strengthening and carbide refinement. The effects of alloying elements on carbide refinement became higher in the order of Cr, Mo, and Mn.
- (3) Increasing the Si content decreased the limiting upsetting ratio of the spheroidized steels. The addition of Mn, Cr, and Mo influenced the limiting upsetting ratio of the spheroidized steels by affecting the morphology of the carbides. The limiting upsetting ratio decreased if many rod-like carbides existed. Micro-cracks formed at the interface between the carbides and ferrite were extended and connected to each other during cold forging, and these then led to macroscopic defects.
- (4) The hardening behavior of normalized steel by induction hardening was able to be interpreted by using the ideal critical diameter. On the other hand, the hardening depth of the spheroidized steels after induction hardening did not always correspond to the ideal critical diameter, and was less than that of the normalized steels.

A decrease in the hardening depth by changing the heat treatment prior to induction hardening from normalizing to spheroidizing annealing was more clearly distinguishable in the Cr-bearing steels, since Cr atoms were dissolved into cementite during spheroidizing annealing, which stabilized the cementite. The cementite was not fully dissolved in the austenite phase by rapid induction heating.

- (5) It can be concluded that a 0.53% C steel can offer the same cold forgeability and induction hardenability that are available from conventional steel for cold forging use by optimizing the chemical composition of the steel on the basis of these results.

References

- 1) H. Sawabe and A. Takahashi: *Sosei-to-Kako (Journal of JSTP)*, 17(1976)187, 644
- 2) Y. Sakamura: *Tokushuko (The Special Steel)*, 29(1980)8, 20
- 3) M. Nagumo, Y. Abe, S. Yamaguchi, K. Oka, M. Akazawa, and H. Nakazima: *Seitetsu Kenkyu*, 274(1972), 1
- 4) M. Kawaberi, H. Imamura, E. Yamanaka, R. Takeda, H. Okumura, and M. Yamaguchi: *CAMP-ISIJ*, 1(1988)2, 510
- 5) H. Hoshi: *Tokushuko (The Special Steel)*, 33(1984)3, 88
- 6) M. Fuzikura: *Denki-Seiko*, 43(1972)3, 149
- 7) K. Osakada, T. Kawasaki, and K. Mori: *Ann. CIRP*, 30(1981)1, 135
- 8) R. Kunitake: "35th Nishiyama Kinen Gijutsu Kouza" ISIJ, (1975), 24
- 9) R. Kunitake: *Journal of JIM*, 32(1968)2, 170
- 10) T. Sato and T. Nishizawa: *Journal of JIM*, 19(1955)6, 385
- 11) C. E. Lacy and M. Gensamer: *Trans. Amer. Soc. Metal.*, 32(1944)38
- 12) T. Shiozaki and T. Kawasaki: *Sosei-to-Kako (Journal of JSTP)*, 27(1986)304, 568
- 13) H. Kawakami, Y. Yamada, T. Kato, and T. Kawasaki: *R&D Kobe Steel Engineering Reports*, 34(1984)1, 73
- 14) B. J. Edlesen and W. M. Baldwin: *Trans. ASM*, 55(1962), 230
- 15) T. Gladman, B. Holmes, and F. B. Pickering: *JISI*, 208(1970), 172
- 16) T. Nakano, Y. Kawatani, and S. Kinoshita: *Tetsu-to-Hagané*, 62(1976)1, 100
- 17) K. Bungard, E. Kunze, and E. Horn: *Arch. Eisenhüttenwesen*, 3(1958)
- 18) T. Nishizawa: *Bulletin of JIM*, 12(1973)6, 401